







Submission to IWMPi 2022

# A drive filter design for MPI with harmonic notching and selective damping

Eli Mattingly <sup>a,b,c,\*</sup>. Monika Śliwiak <sup>b</sup>. John M. Drago <sup>a,b,c</sup>. Erica E. Mason <sup>b</sup>.  
Matthias Graeser <sup>d</sup>. Lawrence L. Wald <sup>a,b,c</sup>

<sup>a</sup>Massachusetts Institute of Technology, Cambridge, MA, USA

<sup>b</sup>Martinos Center for Biomedical Imaging, Massachusetts General Hospital, Charlestown, MA, USA

<sup>c</sup>Harvard Medical School, Boston, MA, USA

<sup>d</sup>Fraunhofer Research Institute for Individualized and Cell-based Medicine, Lübeck, Germany

\*Corresponding author, email: [ematting@mit.edu](mailto:ematting@mit.edu)

© 2021 Mattingly *et al.*;

## Abstract

A harmonically pure and stable drive field is an essential component of any MPI system. Here, we present a filter topology and design methodology tailored for FFL MPI driven at a single frequency. It is a balanced and differential design that minimizes Ohmic losses by transforming the load impedance to a high value for the filtering stages and then back down with a transformer to present an input impedance of  $\sim 6$  Ohms to the drive amplifier. We implement resistors in tuned elements of the drive filter to damp the high-amplitude side resonances these coupled, tuned elements would otherwise generate in the filter design. This helps damp the undesired resonances to avoid noise in the received signal. In addition to the pass-band at the drive frequency, we place notches at the 2nd and 3rd harmonics (total 105dB and 140dB attenuation, respectively) to specifically target these important harmonics. Finally, the circuit elements are picked to maximize stability of the drive current to temperature-induced tuning shifts. The design software (written in Julia), which calculates component values given load parameters and notch locations, has been made available at [OS-MPI.github.io](https://OS-MPI.github.io).

## I. Introduction

With insufficient filtering, the drive amplifier noise and nuisance modulations of its harmonics can easily become the dominant noise source in an MPI system since the magnitude of the drive coil-generated magnetic field is many orders of magnitude stronger than those generated by the SPIONs. Further, drive current drift (magnitude or phase) complicates baseline subtraction procedures and the interpretation of time-series data.

Despite this, there are few complete literature descriptions or design software sources for drive filters optimized with MPI requirements in mind (e.g., extremely low THD, narrow-band, temporal stability). Though, there is some guidance on capacitor selection [1].

Here, we describe a filter topology and method for designing an MPI drive filter and impedance matching structure. Although developed for the example case of a

human brain MPI system [2], the topology and tools are applicable to most other MPI systems.

## II. Methods and materials

The overall filter topology consists of large impedance transformations at the input and output, a narrow-band band-pass filter, and notch filters at select harmonics. Figure 1 shows the four distinct filter sections and the load. From right to left on Figure 1: i) The drive coil and distributed capacitors ii) impedance matching, iii) notching harmonics, iv) band-pass filter, and v) transformer coupling to the amplifier.

**Drive coil:** The load is a series inductor ( $L_{1A/B}$ ), capacitor ( $C_{1A/B}$ ), and resistor ( $R_{1A/B}$ ), where the A/B convention represents the two symmetric elements.

**Impedance matching:** The impedance matching sec-

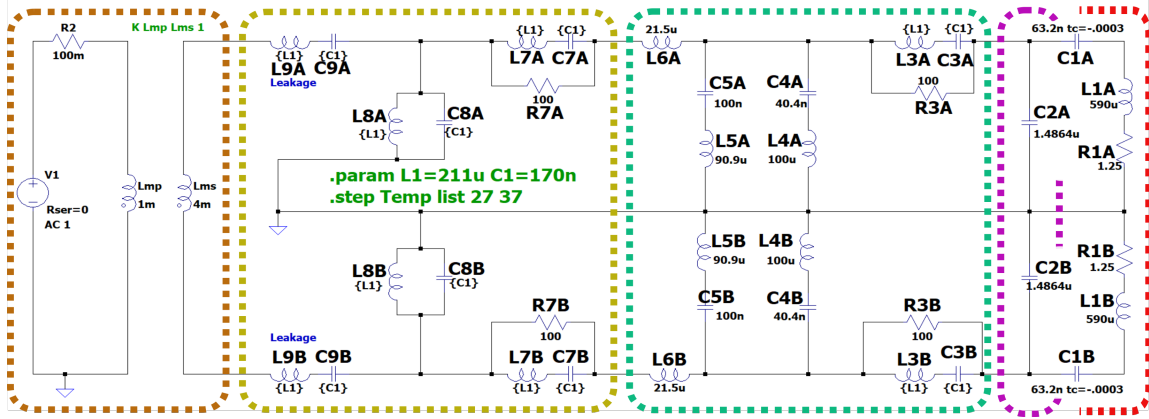


**Figure 1:** The filter topology. The red outlined section is the series LC resonant drive coil with distributed capacitors. The purple outlined section impedance matches each half of the load to a high impedance ( $\sim 12$  Ohms each,  $\sim 24$  Ohms overall) to lower the currents in the up-stream sections. The green outlined section is the notching section aimed at the second and third harmonics and the yellow section is the band-pass section. The orange section depicts the amplifier and a transformer for isolation and unbalanced (amplifier side) to balanced (filter side) impedance transformation to a  $\sim 6$  Ohm load at the amplifier output. Filter inductors have an ESR of 50 mOhms.

tion (purple in Fig. 1) uses C1A/B as well as C2A/B in Fig. 1 to scale the effective impedance of the load. The impedance transformation step reduces the upstream current through the series filter components by a factor of  $\sqrt{m-1}$ , where  $m$  is the matching or transformation ratio. By reducing the current, and therefore the power dissipated in the filter elements, the thermal stability is increased. We chose  $m \approx 10$ .

C1A/B are picked to resonate the drive coil at the drive frequency ( $\sim 26$  kHz in this case), but manufacturing tolerances render this resonance frequency not exactly as designed. This was not considered an issue; instead the inductance and capacitance were measured to determine the drive frequency as:

$$f = \frac{\sqrt{R_f/R_D - 1}R_D + \sqrt{(R_f/R_D - 1)R_D^2 + 4\frac{L}{C}}}{4\pi L} \quad (1)$$

where  $R_f$  is the input impedance into the filter,  $R_D$  and  $L$  is the total drive coil resistance and inductance, and  $C$  is the measured equivalent series capacitance (C1A/B). As long as the Q of the resonant circuit is high the current amplification lead to very low currents in the filter compared to the drive circuit which leads to low losses in the filter.

$R_f$  changes the manner that the current will drift with temperature, as changes in C2A/B (itself a function of  $R_f$ ) will affect the location of the adjacent peaks (at about 26 & 27 kHz in Fig. 2). If the operating point is at the center of these two peaks, both the magnitude and phase are maximally flat. At some ideal  $R_f$ , the drive frequency lands near the mid-point and is maximally stable to thermal (or other) perturbations in capacitor and resistor value changes.

**Targeted damping:** The “targeted damping” places resistors (R3,7A/B in Fig. 1) specifically in pathways

where the current is bypassed by a resonant LC section at the drive frequency. By adding in dissipative elements in this manner, side lobes are heavily attenuated as seen by comparing the dotted and solid trace in Figure 2. This technique can be similarly applied to Rx filter topologies as well to damp unwanted off-resonances. The resistors also reduce the high frequency attenuation, but it is already theoretically well beyond 100dB attenuation.

**Harmonic notching:** “Harmonic notching” (green in Fig. 2) allows for the user to implement notches in the filter response, without adding in any reactance from the amplifier’s perspective. This is done by adding one or more LC shunt sections that resonates at the desired notch frequency. The reactance at the drive frequency added by these shunts is cancelled with a shim inductor (L6A/B) so the amplifier still sees a purely real load. These shunt sections carry very little current because they are relatively high impedance at the drive frequency, and therefore are expected to be very phase and magnitude stable due to the low dissipation.

**Pass-band filter:** The filter section (yellow in Fig. 2) consists of series sections which are resonant at the drive frequency, and shunt parallel L-C sections, which also resonate at the drive frequency. The shunt sections at resonance are ideally infinite impedance, and the series sections at resonance present only the series resistance at resonance, therefore neither add reactance to the network from the input.

**Transformer:** The transformer (orange in Fig. 2) was designed with N87 material (TDK-Lambda, Tokyo, Japan) with two U-shaped core sections (U 141/78/30), which are variably spaced to fine-tune the leakage inductance, which is itself included in the filter. The turn count was picked such that the magnetizing flux is under 10% of the core’s saturation flux (target=25 mT) at full power. By

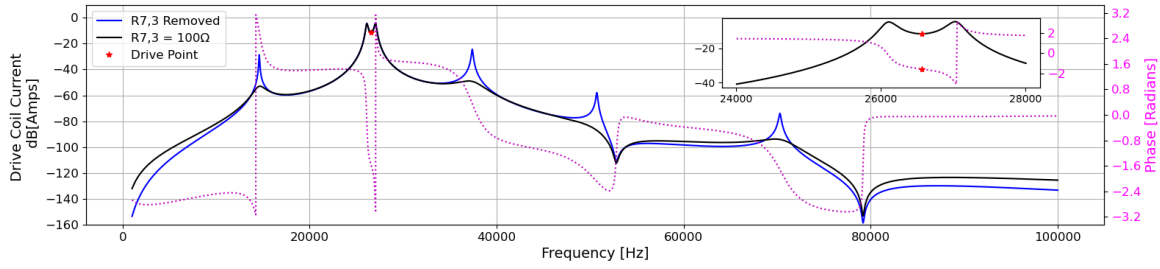


**Figure 2:** Transfer function between input voltage (1 V) and drive coil (L1A/B) current. At the drive frequency, the transconductance is  $\sim 270 \frac{mA}{V}$ . Inset is the same near operating frequency of the damped filter and phase. The blue line is the filter with all the resistors removed. Purple is the phase of the filter with damping (for the damped filter). The driving frequency being halfway between two nearby peaks makes the current less sensitive to perturbations in thermal drifts of the capacitors.

minimizing core flux, the risk of harmonic distortion is mitigated. The transformer acts as a balun to convert the unbalanced output of the amplifier into a balanced source for the symmetric filter design. This provides isolation and rejects common-mode noise and breaks ground loops in the system.

**Inductor cores:** All of the filter inductors (besides the transformer) are air-cored toroids and utilize a D-shaped cross section to maximize the efficiency [3]. The design software package includes a toroid design tool to facilitate the implementation and design of these elements.

### III. Results

The simulated transfer function produced with this filter for a human-scale system is shown in Fig. 2. The insertion loss at the drive frequency is expected to be about -1dB and the attenuation (current relative to the fundamental) at the 2nd, 3rd and 4th harmonics are theoretically about 105dB, 140dB, and 120dB, though it may practically be limited by filter crosstalk. The filter design tool has been made open-source and can be found on OS-MPI.github.io. To run the designer, the functions *DesignDriveFilter(...)*, or for a graphical user interface, *useFilterDesignGUI()* are used, and instructions are found in the README document. This function can build filters with similar topology, for an arbitrary load.

### IV. Discussion and conclusion

The filter topology presented has many advantages over other archetypal designs (e.g. Butterworth, Besel, etc.). First, the notching allows for tremendous attenuation of harmonics (specifically  $2f_0$ ), which would otherwise require numerous, highly dissipative filter stages. This design addition inserts only very low-power sections that are far smaller and easier to implement than making a higher order filter. Secondly, judicious impedance transformations reduce Ohmic heating in the filter.

The drive frequency was placed at the mid-point between the peaks in the transfer function (input voltage

to drive current). While the higher peaks result in more drive current per input volt, they lower overall efficiency. At this center point there is very little drift in output current with thermal drifts in C1A/B (temp. coeff. = -300 ppm per °C). Here (26.57 kHz) the drift given a 10°C rise in C1A/B is about +0.1% in magnitude, and phase drifts 0.45°. At the top of a steep peak (27.03 kHz), the output current will drift dramatically when the capacitors drift with heat: -3.3% magnitude, and 9° phase drift.

The open-source tool for designing similar filters for different loads are available at: OS-MPI.github.io[4].

### Acknowledgements

The authors thank Prof. David Perreault for his helpful conversations regarding filters and Alex Barksdale for his assistance in the lab.

### Author's statement

Conflict of interest: Authors state no conflict of interest. Funding for the work comes from NIBIB U01EB025121, and NSF GRFP 1122374

### References

- [1] B. Zheng, P. Goodwill, W. Yang, and S. Conolly, Capacitor Distortion in Magnetic Particle Imaging, in *International Workshop for Magnetic Particle Imaging*, 319, 2012.
- [2] E. E. Mason, Magnetic Particle Imaging for Intraoperative Breast Cancer Margin Assessment and Functional Brain Imaging, PhD thesis, MIT, 2020,
- [3] P. Murgatroyd and D. Belahrache. D-shaped toroidal cage inductors. *IEEE Proceedings B Electric Power Applications*, 136(2):96, 1989, doi:10.1049/ip-b.1989.0014.
- [4] E. Mattingly, E. E. Mason, K. Herb, M. Śliwiak, K. Brandt, C. Z. Cooley, and L. L. Wald. OS-MPI: An open-source magnetic particle imaging project. *International Journal on Magnetic Particle Imaging*, 6(2):1–3, 2020, doi:10.18416/IJMPI.2020.2009059.